Simulation and characterization of pathway heterogeneity of secondary hydrocarbon migration

Xiaorong Luo

ABSTRACT

Carriers are important links between sources and traps for hydrocarbon migration and accumulation in a petroleum system. Oil and gas commonly migrate along narrow and irregular pathways in porous media, even in macroscopically homogeneous media. A migration simulator based on the invasion-percolation theory, which couples the buoyancy of a hydrocarbon column as the driving force with capillary pressure as the resisting force, satisfactorily explains migration processes in heterogeneous media. In macroscopically homogeneous carriers, migration pathways are generally perpendicular to equipotential lines, but locally, the pathways can be irregular because of the influence of microscopic heterogeneity. The degree of irregularity of these pathways depends on the difference between competing driving and resisting forces. When numerous pathways form in a migration-accumulation system, the flux of migrating hydrocarbons may vary among these pathways. In macroscopically heterogeneous carriers, the irregularity of migration pathways is exacerbated. When the driving force is relatively weak, hydrocarbons tend to migrate in carriers where the hydraulic conductivity is relatively large. These pathways differ from those predicted only on the basis of flow potential. Simulation of the migration process in the Middle Jurassic carrier beds of the Paris Basin demonstrates the characteristics of the migration simulator in the analysis of migration pathway heterogeneity. Results are comparable to or superior to those achieved with previous simulation approaches.

Manuscript received February 25, 2010; provisional acceptance April 29, 2010; revised manuscript received September 16, 2010; final acceptance November 19, 2010.
DOI:10.1306/11191010027

AUTHOR

XIAORONG LUO ~ *Key Laboratory of Petroleum Resources Research, Institute of Geology and Geophysics, Chinese Academy of Sciences, Beijing, China, 100029; luoxr@mail.igcas.ac.cn*

Xiaorong Luo is a research scientist in the Chinese Academy of Sciences and has a B.S. degree and an M.S. degree in geology from Northwestern University, China, and a Ph.D. in geophysics from the University of Montpellier, France. His research interests focus on numerical modeling, geopressuring, and hydrocarbon migration and accumulation.

ACKNOWLEDGEMENTS

This study was supported mainly by the Chinese National Natural Science Foundation (project number 40772090), partly by the Chinese National Major Fundamental Research Developing Project (2006CB202305), and BHP Billiton (L1295XV00). I appreciate the discussions and suggestions from W. Yang of Missouri University of Science and Technology, U.S.A., and G. Vasseur of the University Pierre et Marie Curie, France. W. Yang also helped in English and organization to make this article readable. I thank A. Yu, A. I. Inayat-Hussain, J. Z. Lu, Z. Y. He, and J. C. Liu for their comments and encouragement. I am also grateful for valuable comments and suggestions from three journal reviewers, H. Dembicki Jr., F. Hao, and A. Y. Huc.
The AAPG Editor thanks the following reviewers for their work on this paper: Harry Dembicki Jr., Fang Hao, and A. Y. Huc.

INTRODUCTION

The processes of hydrocarbon migration, accumulation, and dispersal are still not well understood, although understanding the processes is critical to hydrocarbon exploration (Magara, 1978; Chapman, 1982; Ungerer et al., 1990; Mann, 1997; among others). Previous studies on optimal migration pathways in a confined area (Schowalter, 1979; Dembicki and Anderson, 1989; Catalan et al., 1992; Hirsch and Thompson, 1995; Tokunaga et al., 2000; Luo et al., 2004) have improved our understanding significantly. Secondary hydrocarbon migration in carrier beds and reservoirs, after hydrocarbons have been expelled from the source rocks, is a highly heterogeneous process (McNeal, 1961; Harms, 1966; Smith, 1966; Berg, 1975; Schowalter, 1979). Even in macroscopically homogeneous porous media, hydrocarbons migrate along limited pathways that account for only 1 to 10% of the carrier beds in volume (Schowalter, 1979; Dembicki and Anderson, 1989; Catalan et al., 1992; Hirsch and Thompson, 1995; Luo et al., 2007c). In this study, a pathway is defined as the conduit in a carrier bed that may be occupied by migrating hydrocarbons, although the carrier may contain many conduits that are permeable and hydraulically connected and, thus, available for secondary hydrocarbon migration.

At a basin scale, secondary migration pathways may focus in a zone with a size of a few meters (McAuliffe, 1979; Schowalter, 1979; Thomas and Clouse, 1995); and they gradually merge with each other farther away from the source, resulting in a decrease in the density of pathways (Hindle, 1997; Carruthers, 2003; Luo et al., 2007c; Hao et al., 2007, 2009). The heterogeneity of migration pathways is, in essence, an inevitable consequence of hydrocarbons flowing immiscibly within pore water, resulting in unstable digitated clusters.

The complex geometry of pathways is closely related to the heterogeneity of carriers at all scales. At a microscopic scale, the random distribution of pores and pore throats causes an uneven selection of the migration pathway (Lenormand et al., 1988; Hirsch and Thompson, 1995; Tokunaga et al., 2000; Luo et al., 2007a). At a basin or petroleum system scale, lithofacies changes in carriers play an additional important function in causing heterogeneous secondary migration (Weber, 1986; Carruthers, 2003; Luo et al., 2007b), although some authors insist that such changes may not explicitly affect migration pathways (Hindle, 1999; Hao et al., 2007, 2009). Heterogeneity in regional fracture systems was also a factor (Philip et al., 2005); hence, quantitative analysis of hydrocarbon migration should consider not only the driving force, but also the properties and characteristics of carrier beds (England et al., 1987; Bekele et al., 1999; Luo et al., 2007a, b).

Migration is a geologic process that occurs during a long geologic time span. At present, numerical simulation is probably the most effective way to understand the process (Welte et al., 2000; Carruthers, 2003). Several methods have been used to simulate migration processes, including those using principles of flow potential (Hubbert, 1953), multiphase Darcy flow (Ungerer et al., 1990), streamlines (Lehner et al., 1988), flow paths (England et al., 1987; Sylta, 1991; Hindle, 1997), hybrid processes (Bekele et al., 1999), and invasion-percolation (Wilkinson and Willemsen, 1983; Carruthers, 2003). Welte et al. (2000) grouped migration simulation methods into four types: multiphase Darcy flow, flow path or ray tracing, invasion-percolation modeling, and hybrid methods, emphasizing the dynamics of the processes and the scaling or scalability of the data that are critical to modeling efficiency. They suggested that hybrid technologies may eventually combine each individual method into a single integrated tool.

Simulations that rely on these various methods may produce awkward differing results (Shi, 2009), as shown by the discussions between Bekele et al. (1999) and Hindle (1999), on migration pathway simulation in the Paris Basin. It is difficult to determine which method best simulates geologic reality because static data, scaling problems, and hybrid technologies still need to be significantly improved (Welte et al., 2000). Nevertheless, recent studies (Hindle, 1997, 1999; Bekele et al., 1999; Carruthers, 2003; Hao et al., 2007; Luo et al., 2007a, b) indicate that methods based on flow path and invasion-percolation theories may effectively simulate lateral migration at a basin scale.

The invasion-percolation theory (Wilkinson and Willemsen, 1983) has been considered as a dynamic tool to study the displacement of one fluid by another in a porous medium (Furuberg et al., 1988; Meakin et al., 2000). In a model using the invasion-percolation theory, the network has a well-defined sequence of invaded sites, and migrating oil constantly searches for the most favorable breakthrough sites at each step. Furthermore, the invasion-percolation process generates self-similar fractal structures. The basic properties of an invasion-percolation model make it applicable to model the balance between driving and resisting forces under geologically reasonable conditions at the core to basin scale (Carruthers, 2003; Luo et al., 2007a).

In the invasion-percolation models, the migration velocity is assumed to be very slow during basin-scale migration; hence, capillary and buoyancy forces always dominate viscous forces (Carruthers, 2003). A geologic model of a carrier bed can be easily constructed for an invasion-percolation model with limited data because the network possesses a well-defined sequence of sites. Because the buoyancy force may be considered as the major, or even sole, driving force (Wilkinson, 1986), the source of hydrocarbon may be placed at any position in the model, so as to simulate the heterogeneity of source rocks (Luo et al., 2007a, b). The most important advantage of invasion-percolation models is that simple algorithms are used to complete the simulation of hydrocarbon migration in models containing tens or hundreds of millions of grid cells in a matter of minutes (Welte et al., 2000). Having all these properties, invasion-percolation models provide an ideal solution for simulating secondary hydrocarbon migration (Carruthers, 2003; Hantschel and Kauerauf, 2009).

This study uses a migration model based on the invasion-percolation theory to characterize the heterogeneity of secondary hydrocarbon migration pathways and assess the controlling factors. Three factors are identified: nonuniformity of driving force, heterogeneity of carrier beds, and spatial variations in the distribution and amount of expelled hydrocarbons from source rocks. Simulation of the migration process in the Middle Jurassic carrier beds of Paris Basin is used to demonstrate the characteristics of our invasion-percolation model in the analysis of migration pathway heterogeneity.

METHODOLOGY

Our previous physical experiments (Zhang et al., 2003; Luo et al., 2004; Hou et al., 2005) have identified three patterns, namely stringer, finger, and piston, of hydrocarbon migration pathways, among which stringers dominate when buoyancy is the main driving force under realistic basin-scale conditions. Based on the current understandings about secondary migration of hydrocarbon in carriers, as reviewed by Carruthers (2003) and Hao et al. (2007), results of our physical models and those of Hirsch and Thompson (1995) and Ewing (1997) are used to establish an invasion-percolation–based numerical model, termed the MigMOD model (Bo et al., 2006; Luo et al., 2007b). This model consists of 2-D networks where the nodes represent pores and the links represent the throats in a carrier. The radii of pores and throats are assigned by a random-number generator that follows a Gaussian distribution, and the mean and standard deviation change according to the lithologic characteristics of the carrier.

In invasion-percolation models, buoyancy force as the driving force and capillary force as the resisting force are always present during hydrocarbon migration. Hence, a dimensionless parameter can be used to represent the relationship between the two forces. The dimensionless Bond number (B_o) of Wilkinson (1986) describes the relationship between buoyancy and capillary forces at the scale of pores:

$$B_o = \frac{(\rho_w - \rho_o) g r^2}{2\sigma} \qquad (1)$$

where r is the radius of the pore throat; ρ_w and ρ_o are densities of water and oil, respectively; g is the gravitational acceleration; and σ is the interfacial tension between water and oil.

The heterogeneity of hydrocarbon migration in carrier beds can be analyzed in three ways (cf. Luo et al., 2004, 2007a, b, c). First, at each step of simulation, migrating hydrocarbon breaks through

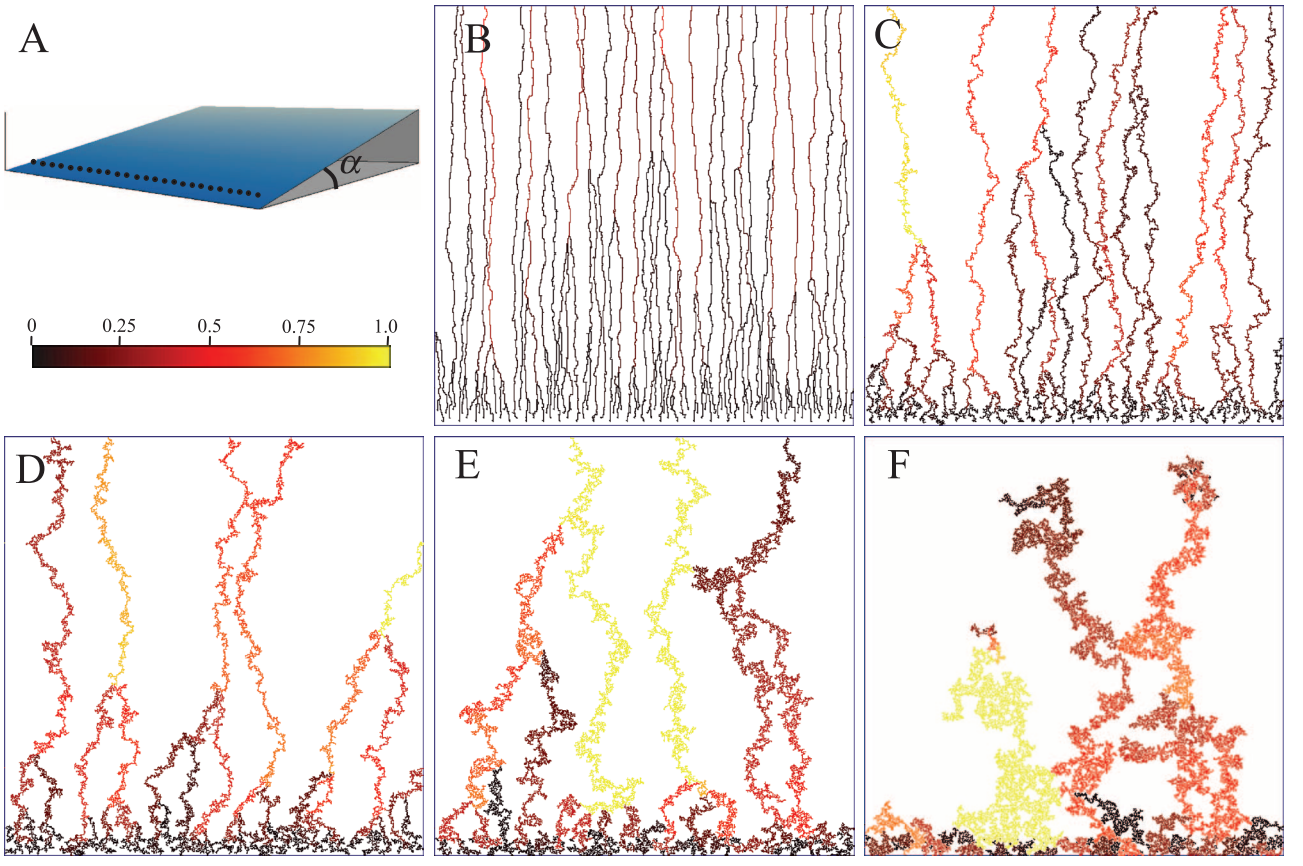

Figure 1. Simulation of hydrocarbon migration pathways in an inclined plate composed of a macroscopically homogeneous medium in a uniform flow-potential field. (A) The inclined plate with a dip angle 5.72°. Dots along the base line show the position of hydrocarbon injection points. The color bar scale is the relative flux of migrated oil in pathways for simulation results in panels B to F. The scale also applies to simulation results in subsequent figures. (B–F) Results of simulated pathways with Bond numbers 1.0×10^{-1}, 1.0×10^{-2}, 1.0×10^{-3}, 1.0×10^{-4}, and 1.0×10^{-6}, respectively. Numbers along the horizontal and vertical axes are grid coordinates. Oil is injected along a zone of 20 × 500 sites at the base of the plate. The density of the injecting zone is one inject point every 10 × 10 sites.

at a pore throat where the difference between driving and resisting forces is the largest. A new pathway forms and extends step by step. Second, migrating hydrocarbons do not occupy all existing pathways, that is, existing pathways are not associated with the same flux of hydrocarbons. Instead, hydrocarbon migrates, within existing pathways, selectively along the points with a relatively large difference between driving and resisting forces. Last, the flux of hydrocarbon through a given pathway is dependent on the amount of hydrocarbon supply from the connected source rocks, which varies within a source rock area. To illustrate the varying amounts of migrating hydrocarbon along pathways, this study considers the combined effects of driving and resisting forces, properties of carrier beds, and rate of hydrocarbon supply. This is accomplished by assigning specific hydrocarbon expulsion rates and amounts from the source rock and registering and color coding the amount of migrated hydrocarbon crossing each grid point in the carrier bed. The heterogeneity of migration is shown by the varying width of pathways and varying flux of hydrocarbons within the pathways (Figure 1).

Considering that snap-off and segmentation are common processes in heterogeneous porous media during hydrocarbon migration (Carruthers, 2003), our model establishes the following rules: (1) A migrating hydrocarbon segment always breaks through the throat where the difference between driving and resistant forces is the largest among all the throats along the oil-water boundary; and (2) if the driving force at all boundary throats is not large enough to make a hydrocarbon segment break

through any throat, the segment stays and waits for a following segment to form a new amalgamated segment. This combining process repeats until the hydrocarbon segment is long enough to break through a boundary throat. However, the height of the amalgamated segment cannot grow infinitely and is limited as

$$H_{\text{lim}} = \text{P}_{\text{cris}}/\Delta\rho g + \delta P/\rho_{\text{w}} g \qquad (2)$$

where P_{cris} is the percolation pressure of a carrier (Hantschel and Kauerauf, 2009), $\Delta\rho$ ($= \rho_{\text{w}} - \rho_{\text{o}}$) is the water-oil density difference, and δP is the pressure difference between a source rock and the carrier. Such a design permits us to simulate some cases where the driving forces in hydrocarbon sources are smaller than capillary pressures of carriers, so that hydrocarbon may not migrate in carriers.

In fact, a specific pore-throat radius requires a minimum height of a migrating hydrocarbon segment for it to break through the throat because the segment with the minimum height will generate a buoyancy force equal to the capillary pressure of the throat. In our model, once a hydrocarbon segment breaks through a throat, it flows directly to the next pore, regardless of the distance between two pores. This rule implies that the pattern of simulated pathways also depends on the vertical distance between two grid nodes (i.e., the vertical scale) of a simulator grid.

For most simulation cases presented in this article, the density difference between oil and water is $0.2\ \text{g} \times \text{cm}^{-3}$, surface tension between oil and water is $40\ \text{dyne} \times \text{cm}^{-1}$, and the gravitational acceleration is $9.80\ \text{m} \times \text{s}^{-2}$. The variation of Bond number is realized by assigning different average radii of throats. The average radii of pore throats are assigned as 2.0, 0.63, 0.20, 0.063, 0.02, and 0.0063 mm, which correspond to Bond numbers 10^{-1}, 10^{-2}, 10^{-3}, 10^{-4}, 10^{-5}, and 10^{-6}, respectively.

HETEROGENEITY OF MIGRATION PATHWAYS AND ITS CONTROLLING FACTORS

The heterogeneity of migration pathways at a basin scale is analyzed through progressively complex simulations. The simulations individually demonstrate the effect and control of the heterogeneous driving force and properties of carrier beds and source rocks on pathway formation and heterogeneity. The composite effect of simple combinations of these individual factors is also presented.

Pathway Heterogeneity in Homogeneous Carrier Beds in a Uniform Flow-Potential Field

A porous medium is statistically defined as macroscopically homogeneous but microscopically heterogeneous if the radius of pore throats follows a specific probability distribution (Gaussian distribution in this study). A uniform flow-potential field is characterized by parallel and equally spaced equipotential lines. Fluid dynamics analysis of this model through simulation on the basis of hydraulic potential or Darcy's law shows that flow pathways are perpendicular to equipotential lines (Allen and Allen, 1990; Hindle, 1997).

Inclined Plate

An inclined plate can be defined as $z = Cy$, where y and z are the coordinates in the dip and vertical directions, respectively; C is the dip angle, which determines the magnitude of buoyancy force (Figure 1A). The plate was covered by a 500×500 grid, and oil injected along a zone of 20×500 sites at the base of the plate migrates upward under buoyancy force. The density of injecting zone is one inject point every 10×10 sites. Different pathways form, corresponding to different Bond numbers (Figure 1B–E).

The simulation indicates that the ratio between driving and resisting forces controls the pathway geometry in the porous medium of a given pore-throat size distribution. In the case of a relatively large driving force (i.e., a large ratio between driving and resisting forces; $B_0 = 10^{-1}$; Figure 1B), pathways are generally perpendicular to the equipotential lines, and pathways originated from individual injection points are separated. Migration appears to have an overall homogeneous pattern. With a decreasing driving force (Figure 1C), however, pathways become irregular; and pathways

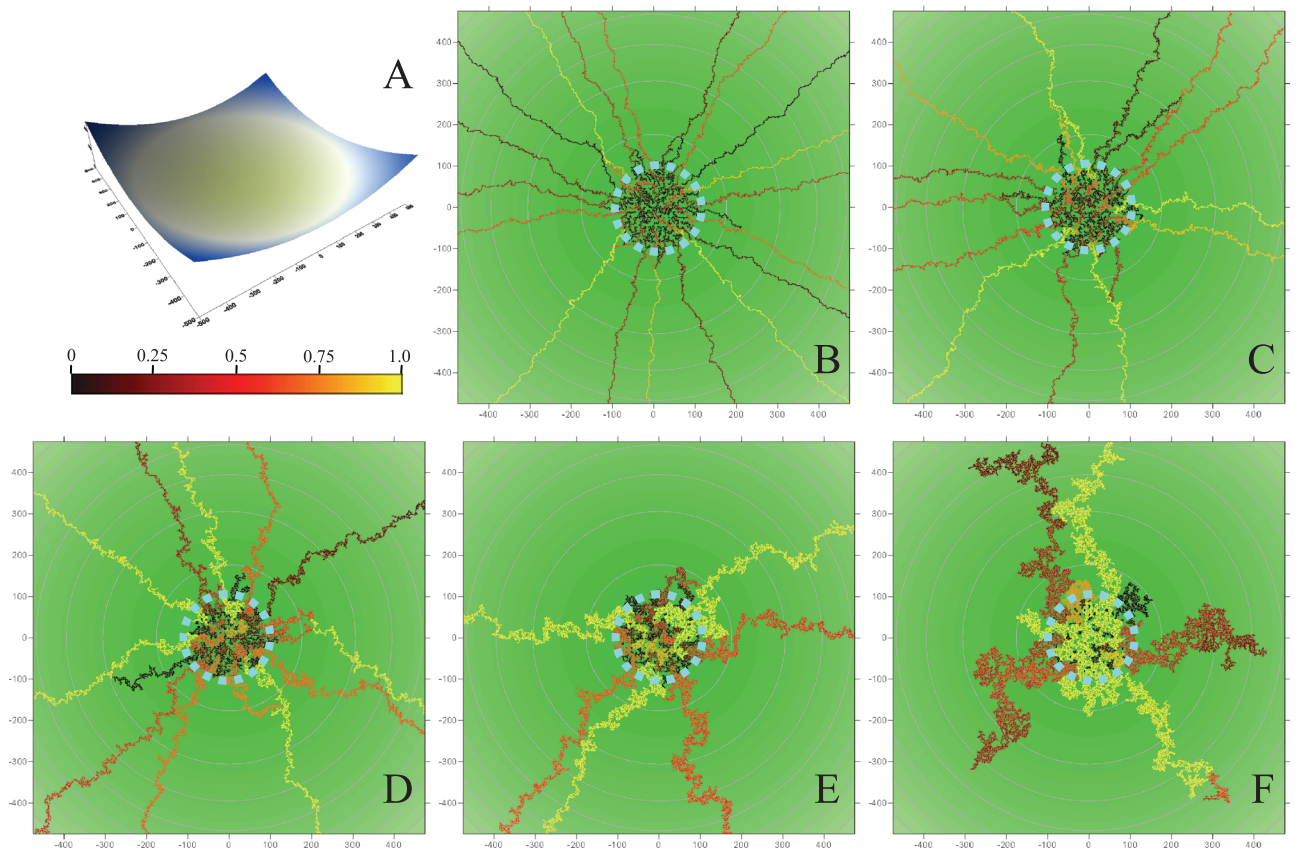

Figure 2. Simulation of pathways in a circular syncline composed of a macroscopically homogeneous medium in a uniform flow-potential field. (A) The circular syncline created by a rotating hyperbolic surface ($z = 0.01\ [x^2 + y^2]$). Three-dimensional grid axes are shown. The color bar scale is the same as in Figure 2. (B–F) Results of simulations with Bond numbers 10^{-2}, 10^{-3}, 10^{-4}, 10^{-5}, and 10^{-6}, respectively, where numbers along the horizontal and vertical axes are grid coordinates; oil is injected within the green circle at the center of the syncline and migrates outward from the center to the edge.

originated from different injection points merge to form a rootlike network with a general direction perpendicular to the equipotential lines. Nevertheless, all pathways appear evenly distributed on the plate. With a further decrease in the driving force (Figure 1D), pathways become more complex, their average width increases, and pathways from different injection points merge extensively, resulting in only a few of the pathways reaching the top of the plate. The overall migration direction is perpendicular to the equipotential lines, but locally, migration direction is not controlled by the direction of the driving force. The amount of migrating hydrocarbon varies among pathways. Finally, when the driving force is very weak (Figure 1E, F), pathways originating from individual injection points merge easily. As a result, the number of pathways is small, and pathways form patchy networks and are not perpendicular to equipotential lines.

Symmetrical and Circular Basin

A symmetrical and circular basin is the other simple basin type under a uniform flow-potential field (Pratsch, 1983). This model has a hyperbolic surface (Figure 2A). Homogeneous pathways are mostly perpendicular to equipotential lines and do not merge with each other, when the driving force is much larger than the resisting force (Figure 2B). With a relative increase of resisting force, random switching of pathways becomes frequent to cause pathway merge, an increase in the width of pathways, and a reduction in the number of pathways (Figure 2C–E). Overall, the pathway characteristics

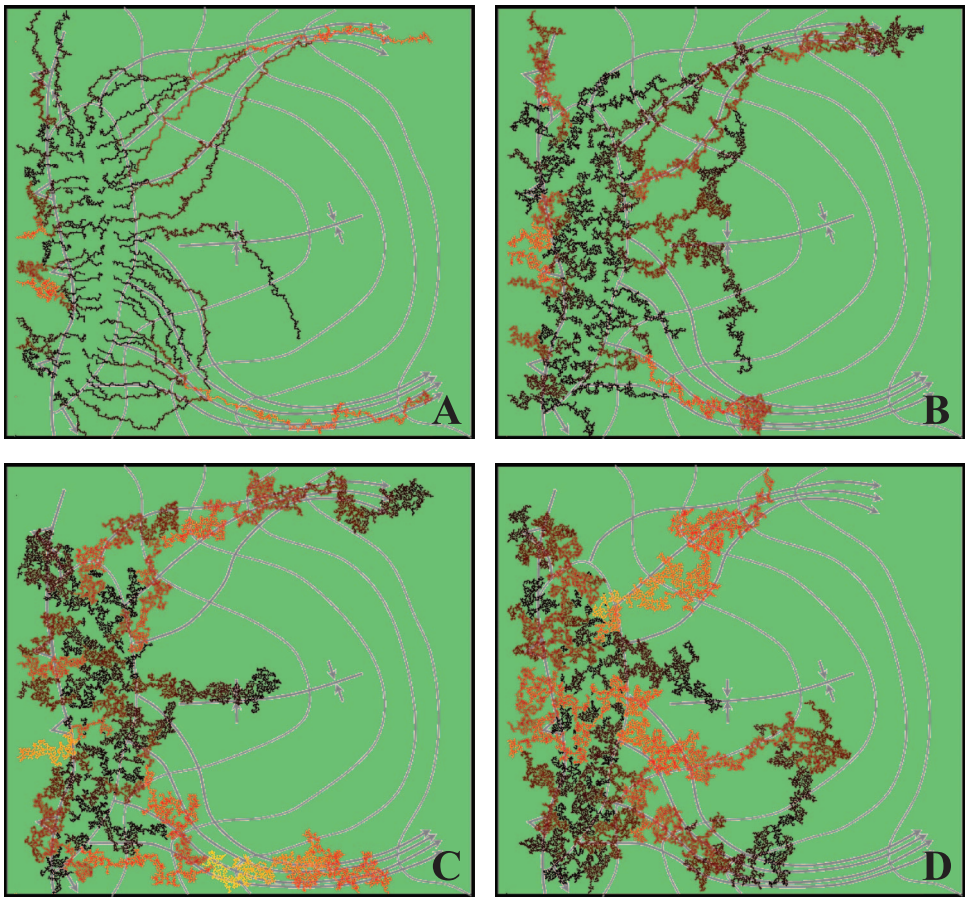

Figure 3. Simulation of pathways in a conceptual foreland basin of Allen and Allen (1990). The thrust load is located at the leftmost edge, and the foredeep and source rock kitchen are next to the thrust load in the model. Two structural backbones extend into the kitchen. (A–D) Results of simulations with Bond numbers 10^{-2}, 10^{-3}, 10^{-4}, and 10^{-5}, respectively. Contour and flow lines are from Allen and Allen (1990).

corresponding to various Bond numbers are similar to those in the inclined plate model (Figure 1).

Conceptual Foreland and Elliptic Basins

In the case where groundwater circulation can be neglected, the driving force is buoyancy, so that the migration pathways are controlled by the geometry of a basin (Allen and Allen, 1990; Hindle, 1997; Hao et al., 2007, 2009). Oil expelled from source rocks migrates laterally toward areas of a low-flow potential (Allen and Allen, 1990; Hindle, 1997), that is, migration pathways tend to appear where flow lines are concentrated (Figures 3, 4).

Allen and Allen (1990) discussed migration in conceptual foreland and elliptic basins. They demonstrated two modes of migration: a converging mode in foreland basins and a diverging mode in elliptic synclines. In our simulation using the two conceptual basin models, a network of 350,000 nodes is used for both models to balance model details and calculation capacity. The pore size in the carrier follows the normal distribution. Buoyancy is determined by the density difference between water and oil and topography at the top of the carrier bed.

For the foreland basin model, many migration pathways occur in the source area and merge toward and along the structural backbones, when B_o is large (Figure 3A). The pathways match the flow lines, and the heterogeneity of the pathways is not significant, although all the pathways merge on the structure backbones. With a decrease in B_o, pathways widen, and the distribution and flux of oil within pathways become more heterogeneous (Figure 3B–D). When $B_o \geq 10^{-4}$, oil migrates along the structure backbones, suggesting that the heterogeneity of pathways does not change the general migration direction. When $B_o < 10^{-5}$, however, pathways do not have a dominant direction because oil migration is equally controlled by the driving force and the resistant force.

For the elliptic syncline model, dominant pathways occur mainly in the direction of the short axis

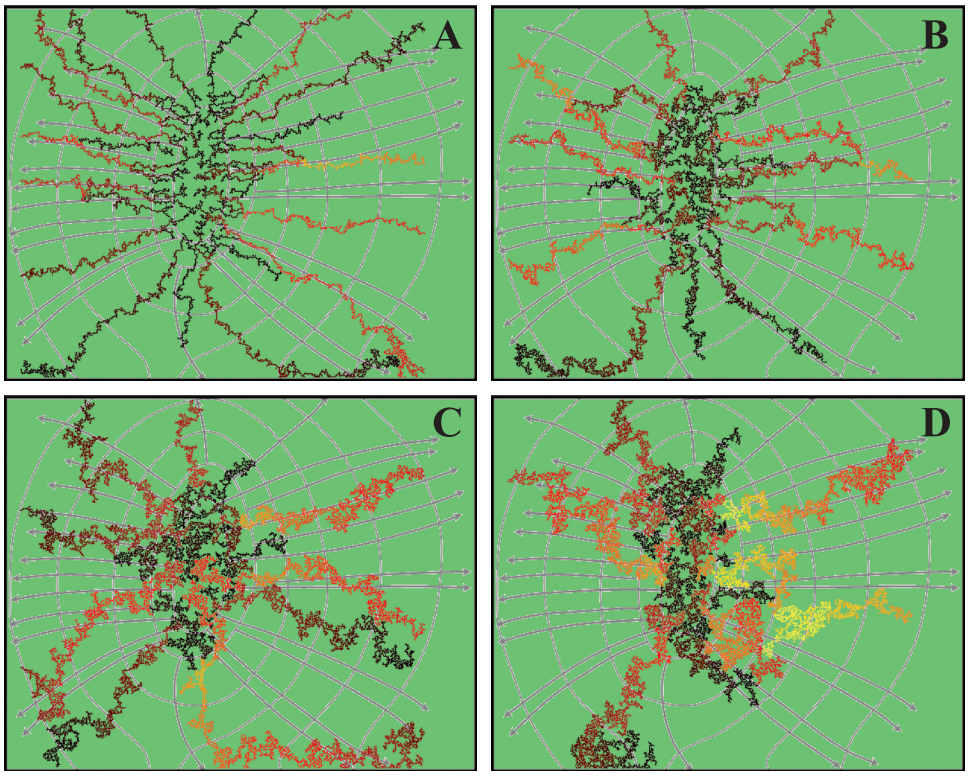

Figure 4. Simulation of pathways in a conceptual elliptic syncline model of Allen and Allen (1990). The long axis of the basin is oriented north to south. (A–D) Results of simulations with Bond numbers 10^{-2}, 10^{-3}, 10^{-4}, and 10^{-5}, respectively. Contour and flow lines are from Allen and Allen (1990).

(Figure 4A) when B_o is large. The concentration of pathways is controlled mainly by the flow potential field. However, with a decrease in B_o, the distribution and flux of oil within pathways become increasingly heterogeneous (Figure 4B–D).

Pathway Heterogeneity in Macroscopically Homogeneous Carrier Beds in a Uniform Flow-Potential Field as Caused by a Heterogeneous Hydrocarbon Source

In the following simulations, the position and geometry of source rock areas vary and do not coincide with the center of synclines. In addition, the amount of expelled hydrocarbon from source rocks varies within source rock areas. The variation is characterized in this study by the expulsion intensity, which is defined as the amount of hydrocarbon expulsion from source rocks within a unit of source rock area over the period of migration.

Source Rock Area Offset from the Center of a Syncline

When the source rock area does not coincide with the center of a syncline, pathways tend to concentrate at the side of the source rock (Figure 5B; compare with Figure 5A). With an increasing offset, the pathways become increasingly confined to the limb; where the source rock is located, so is the amount of migrated hydrocarbon.

Change of Hydrocarbon Expulsion Intensity

The amount of hydrocarbons expelled varies from location to location within a source area because the source rock varies laterally in quality, quantity, and maturity (Bekele et al., 1999). Thus, two simple scenarios of nonuniform expulsion intensity are simulated to assess the effect of changing hydrocarbon expulsion intensity. In the first scenario, hydrocarbon is expelled from the center of a syncline (Figure 5C), where expulsion intensity is doubled in a small area that is offset from the center of the syncline within the source area. The results show that the number of pathways does not change (compare with Figure 5A), but the amount of migrated hydrocarbons in individual pathways increases at the side with relatively large expulsion intensity (Figure 5C). In the other scenario, where a part of the source area does not expel any hydrocarbon, both the number of pathways and the amount of migrated hydrocarbons in individual

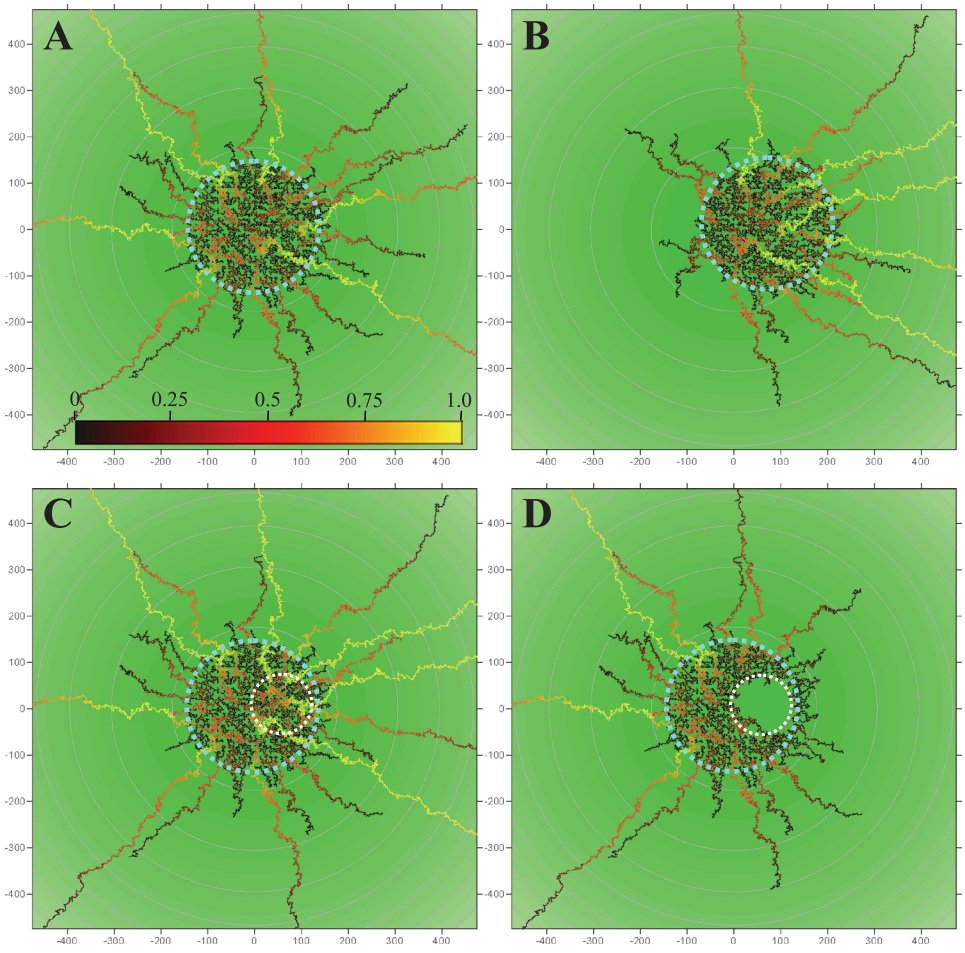

Figure 5. Simulation of pathways in a circular syncline composed of a macroscopically homogeneous medium in a uniform flow-potential field with different source rock locations. The configuration of the syncline is the same as that in Figure 2. The Bond number is 10^{-2}. (A) The source rock area (outlined by a dashed blue circle) lies in the center of the syncline. Oil is injected uniformly over the source area and migrates outward. (B) The source rock area shifts from the center of the syncline upslope at an increment of 0.5R (R = radius of the source rock area). (C) Configuration of a circular syncline similar to that in panel A. However, the intensity of oil expulsion within the white circle is doubled to simulate a nonuniform source area. (D) Configuration of a circular syncline similar to that in panel A. However, the intensity of oil expulsion within the white circle is null to simulate a nonuniform source area. Numbers along the horizontal and vertical axes are grid coordinates on the *xy* plane, and the *z* coordinate is not shown. Thin faint gray circles are topographic contour lines. Color bar scale is the relative flux of migrated oil in pathways.

pathways decrease at the side with reduced expulsion intensity (Figure 5D).

Pathway Heterogeneity Within a Heterogeneous Carrier Bed

Carrier beds are inherently heterogeneous (Weber, 1986). The heterogeneous physical properties of carrier beds play a significant control on the selection of breakthrough points by migrating hydrocarbons (Bekele et al., 1999).

Simple Heterogeneous Carrier Beds

The carrier bed in a hyperbolic syncline (Figure 6) is subdivided into eight octants. Each octant consists of one of three types of carriers. The average pore-throat radii of the three types of carriers are assigned as 0.63, 0.2, and 0.063 mm with standard deviations of 0.31, 0.1, and 0.031 mm, respectively. These parameters correspond to B_o values of 10^{-2}, 10^{-3}, and 10^{-4}.

When the buoyancy force dominates, as simulated by an order of increase in the Bond number,

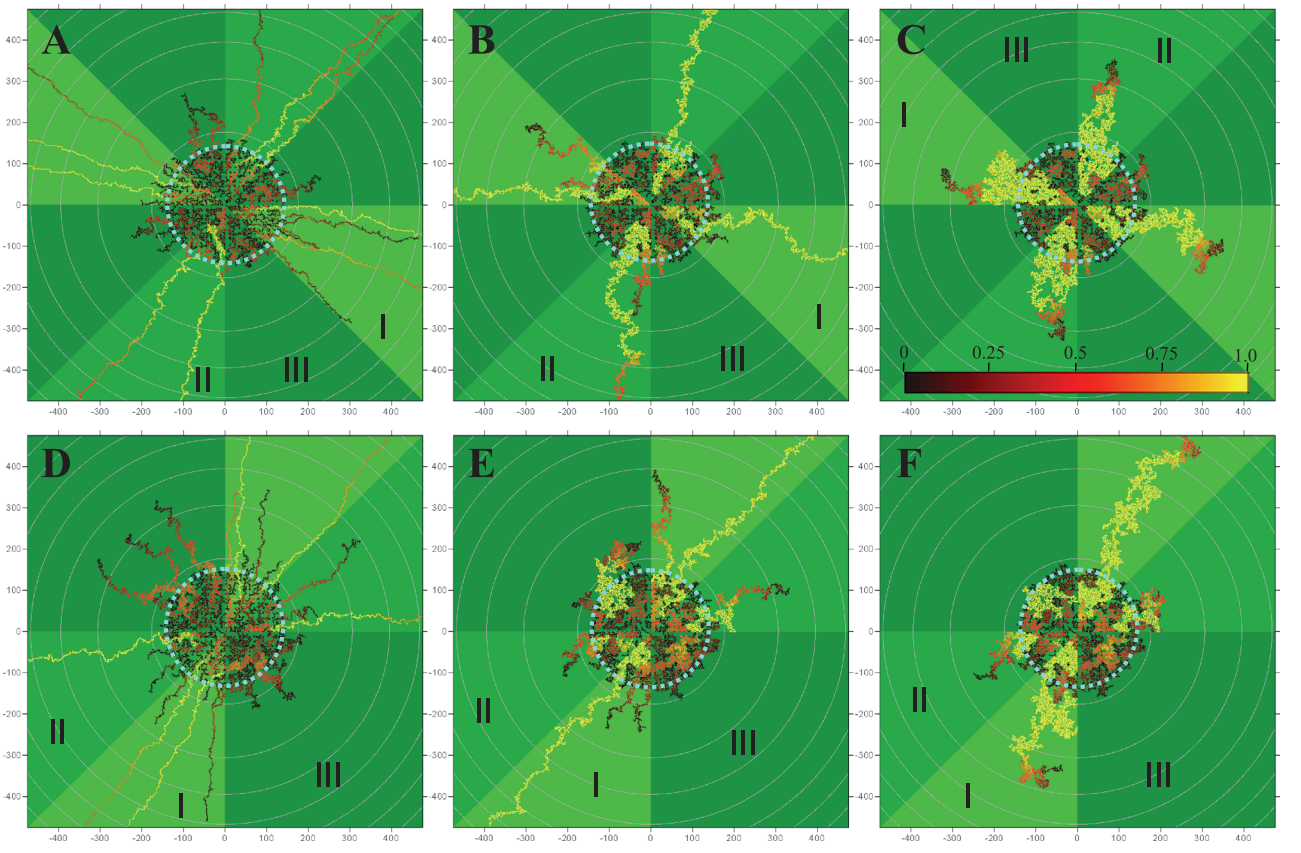

Figure 6. Simulation of pathways in a circular syncline composed of macroscopically heterogeneous carriers in a uniform flow-potential field. Configuration of the syncline is the same as that in Figure 5A. The color bar scale in panel A is the relative flux of migrated oil in pathways, and the dashed circle in the center outlines the source area. The carriers have three types: types I, II, and III carriers have an average pore-throat radius of 0.63, 0.2, and 0.063 mm, with a standard deviation of 0.31, 0.1, and 0.031 mm, respectively. (A–C) The three types of carriers alternate with each other, and four type III carriers separate types I and II carriers. (D–F) The three types of carriers alternate with each other, and types I, II, and III carriers are arranged counterclockwise so that a type I octant will be adjacent to a type II octant at one side and to a type III quadrant at the other side. Oil is injected uniformly over the source area and migrates outward. The bond number decreases 10 times in panels A and D and increases 10 times in panels C and F. Numbers along the horizontal and vertical axes are grid coordinates on the *xy* plane, and the *z* coordinate is not shown. Thin light green circles are topographic contour lines.

the impact of carrier bed heterogeneity on pathway formation is minimal. The pathways extend in all directions with equal chances and are narrow (Figure 6A). However, the pathways in three types of carriers differ significantly. In type I carriers, pathways are narrow, long, and numerous. In type II carriers, pathways are wide and merging with each other. In type III carriers, migration is sluggish, forming only one or two short pathways. Considering the effect of expulsion intensity on migration pathways as illustrated in Figure 5A, the lack of pathway development in type III carriers may be caused by preferential migration in types I and II carriers with larger pore throats and, thus, larger Bond numbers.

The competition among different types of carriers intensifies with increasing Bond numbers. Migration is limited in type III carriers within the source area; oil is concentrated in a few pathways in types I and II carriers (Figure 6B). To the extreme case where the resisting force dominates, most migration occurs along pathways in types I and II carriers (Figure 6C). Furthermore, pathways in types I and II carriers have similar characteristics when they are separated by type III carriers (Figure 6A–C). The reason is likely that type I or II carriers are always preferential migration media in comparison with adjacent type III carriers. However, when types I and II carriers are adjacent to each other at one side and to a type III carrier at the other side (Figure 6D–F),

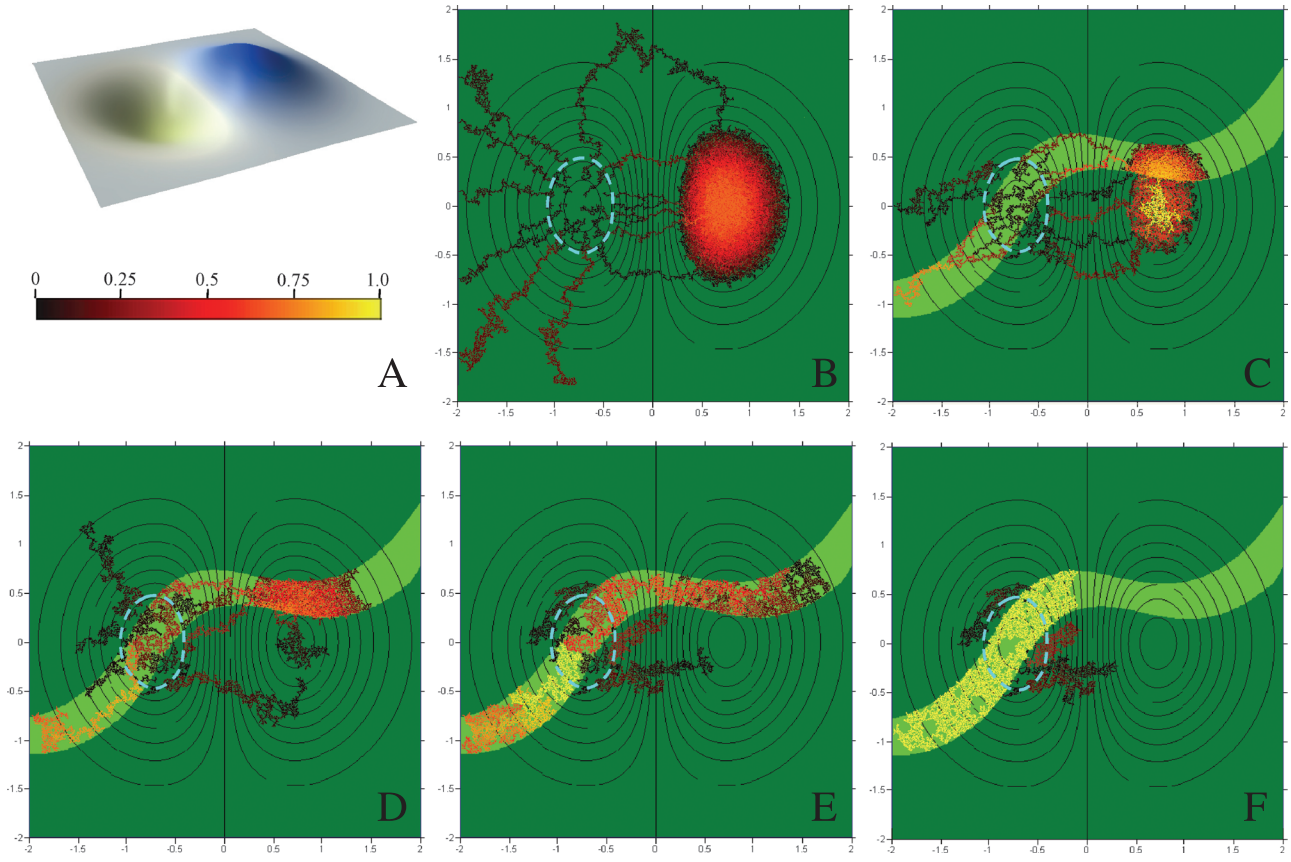

Figure 7. Simulation of pathways in an adjoining syncline and anticline composed of macroscopically heterogeneous media in a uniform flow-potential field. (A) Structural configuration of the adjoining syncline (lower left) and anticline (upper right) constructed using $z = x \times \mathrm{EXP}(-x^2-y^2)$. The color bar scale is the relative flux of migrated oil in pathways. (B) Simulation results corresponding to a Bond number of 1.0×10^{-3} with a homogeneous carrier medium with an ellipse as the source area. (C–F) The meandering carrier bed has an average pore-throat radius of 0.2 mm, with a standard deviation of 0.1 mm, and the channel sandstone has an average pore-throat radius of 0.63 mm, with a standard deviation of 0.31 mm. Simulation results with the meandering carrier bed corresponding to Bond numbers 1.0×10^{-3}, 1.0×10^{-4}, 1.0×10^{-5}, and 1.0×10^{-6}, respectively. And the values of Bond number corresponding to the channel sandstone are 1.0×10^{-2}, 1.0×10^{-3}, 1.0×10^{-4}, and 1.0×10^{-5}, respectively. Numbers along the horizontal and vertical axes are grid coordinates on the *xy* plane, and the *z* coordinate is not shown. Thin black circles are topographic contour lines and labeled with elevation.

competition between types I and II carriers for preferential migration within the source area occurs. Type I carriers win the competition, as shown by the abundant pathways in type I carriers and limited pathways in type II carriers (Figure 6D–F). As the area of type III carriers increases in the basin, migration becomes more important in type III carriers (Figure 6D, E).

Irregular Linear Carrier Beds across an Adjoining Syncline-Anticline

A curving carrier bed simulating a permeable meandering channel sandstone is superimposed on a syncline-anticline structure (Figure 7A). The meandering bed has an average pore-throat radius of 0.63 mm, with a standard deviation of 0.31 mm, that correspond to a Bond number of 10^{-2} (Figure 7C), whereas the carrier beds outside the meandering belt have an average pore-throat radius of 0.2 mm, with a standard deviation of 0.1 mm, corresponding to a Bond number of 10^{-3} (Figure 7C). A source area is located around the center of the syncline and is slightly larger than the width of the meandering belt. Thus, most of the expelled hydrocarbons enter the meandering sandstone and a small part enters into the adjacent low-quality carrier bed. For comparison of pathway heterogeneity between homogeneous and heterogeneous carrier

beds, migration in a macroscopically homogeneous carrier bed in the same syncline-anticline is simulated (Figure 7B). In the homogeneous model (Figure 7B), the average pore-throat radius is 0.2 mm, with a standard deviation of 0.1 mm, corresponding to a Bond number of 10^{-3}.

Migration pathways are controlled by the meandering carrier bed (Figure 7C–F). Hydrocarbons trapped initially in the meandering belt can only migrate within the belt. Pathways in the low-quality carrier bed, once intercepting the meandering belt, also enter the meandering belt. In the case of large Bond numbers (Figure 7C), pathways are narrow as controlled dominantly by the buoyancy force, and are abundant outside the meandering belt, indicating a weak control of carrier bed heterogeneity. Nevertheless, in comparison with the simulation result with a homogeneous carrier bed (Figure 7B), pathways in the upper slope are affected to a certain degree by the presence of the meandering belt. In addition, hydrocarbon accumulates in two separate traps at the top of the anticline, one outside the meandering belt, the other within the belt in a nose structure (Figure 7C). When the nose structure is filled up, some hydrocarbons spill over the meandering belt into the adjacent trap.

The impact of heterogeneity of the carrier beds increases when the Bond number decreases. Pathways increasingly converge toward and merge into the meandering belt and widen. As a result, a lesser amount of hydrocarbons is available to charge directly to the anticline outside the meandering belt. When the Bond number is 10^{-5} in the meandering belt and 10^{-6} outside the belt, most of the pathways are confined in the meandering belt, deviating from the direction of the driving force (Figure 7F). In addition, pathways outside the meandering belt are widened and more prone to intercept and merge with the meandering belt and, as a result, do not extend far upslope.

PATHWAY HETEROGENEITY IN THE PARIS BASIN

Migration pathways in the Paris Basin are analyzed to test and improve the insights gained through aforementioned simulations. The Paris Basin is selected because of its laterally continuous carrier beds, relatively simple structural configurations, and well-studied hydrocarbon systems (Chiarelli, 1973; Pages, 1987). In addition, Hindle (1997) and Bekele et al. (1999) have conducted simulations of hydrocarbon migration pathways. Bekele et al. (1999) specifically emphasized the migration heterogeneity associated with the Jurassic Dogger Formation. Hindle (1997) applied a flow path method in his simulation, and Bekele et al. (1999) used a hybrid method. Thus, it will be interesting to compare my results with those of previous studies.

The Paris Basin in northern France is a Mesozoic–Cenozoic cratonic interior basin, covering 50,000 km^2. Sedimentary deposits in the basin center are 3000 m (9843 ft) thick and include mainly Mesozoic and Tertiary siliciclastic rocks intercalated with carbonate rocks. Hydrocarbons discovered in Triassic, Middle Jurassic, and Lower Cretaceous rocks account for, respectively, 50, 40, and 10% of the total discovered hydrocarbons in the basin (Hindle, 1997). Model results of Hindle (1997) and Bekele et al. (1999) indicate that the Lower Jurassic source rocks matured and hydrocarbon was expelled during the Cretaceous–Oligocene (Espitalié et al., 1988), when the structural configurations of seal beds capping Middle Jurassic carrier beds started to stabilize.

In this study, the geologic migration models of Hindle (1997) and Bekele et al. (1999) are used, including the present structural configuration at the top of the Middle Jurassic carrier bed, hydrocarbon discoveries (Figure 8A), the rate of hydrocarbon expulsion from the Lower Jurassic source rocks to the Middle Jurassic carrier bed (Figure 8B), and basin-scale permeability variations of the Middle Jurassic carrier bed (Figure 8D, E). Numerical simulation is conducted using the MigMOD computer codes of Luo et al. (2007b).

The area in this study is covered by a 600 × 590 grid. The Middle Jurassic carrier beds were considered as uniform (Hindle, 1997) (Figure 8C) or subdivided into three types with distinctive ranges of permeability (Figure 8D). The expected value of pore-throat distribution (r) is obtained from the average permeability of three types of carrier beds

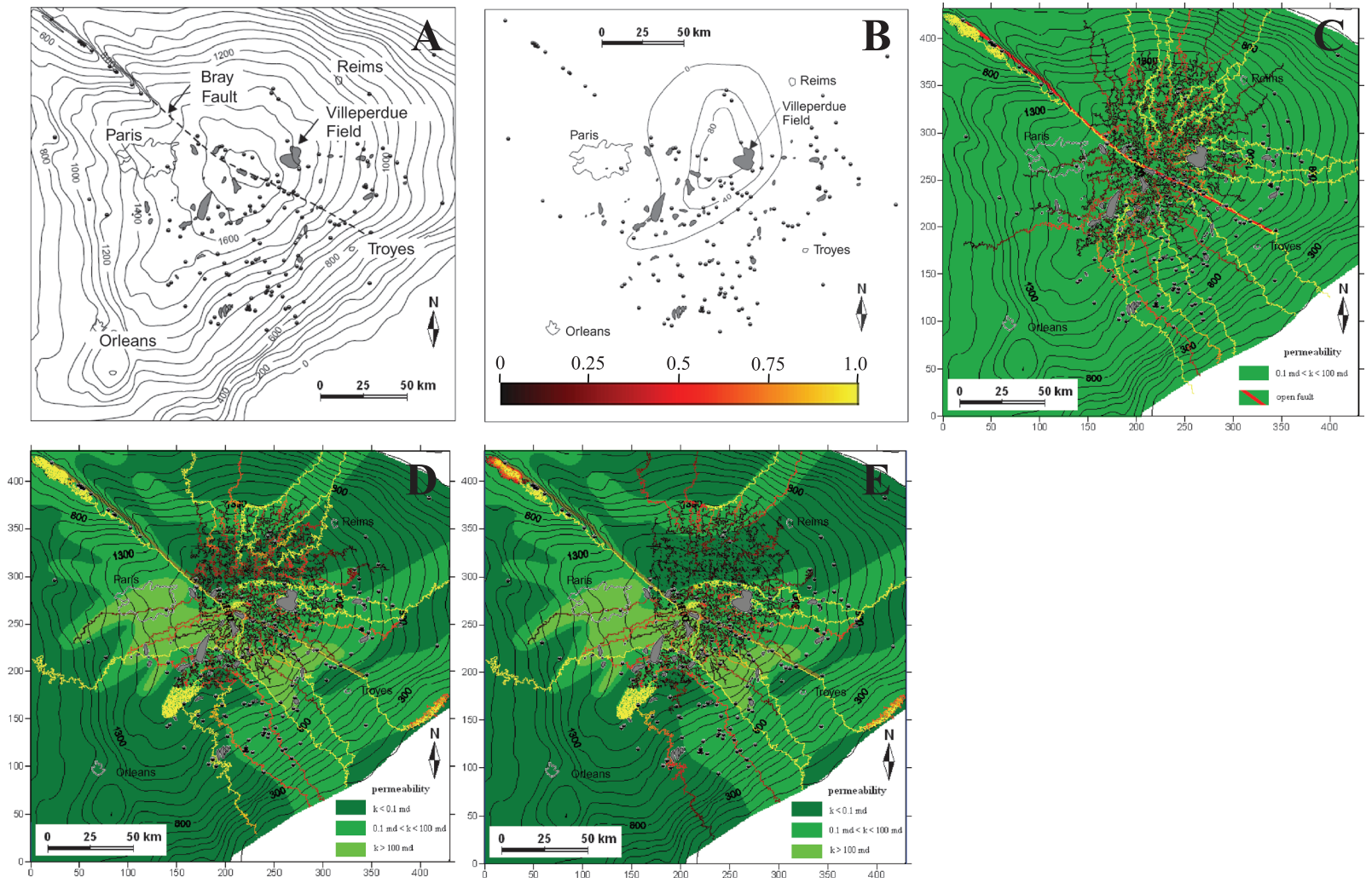

Figure 8. Simulation of migration pathways in the Dogger Formation of the Paris Basin. (A) Schematic map showing the structure map at the top of the Middle Jurassic Dogger Formation with depth in meters, the Bray fault, and the discovered oil fields. (B) Map showing the intensity of expelled oil from the Lower Jurassic source rock underlying the Dogger Formation. Modified from Hindle (1997) and Bekele et al. (1999). (C) Simulation result of pathway development in the Dogger Formation with a uniform carrier bed, where the permeability is assumed to be 10 md. The blue line is the Bray fault, which was open during secondary migration. (D) Simulation result of pathway development in the Dogger Formation with a heterogeneous carrier bed, where the average permeabilities of the three types of reservoirs are 150, 10, and 0.1 md, respectively. (E) Simulation result of pathway development in the Dogger Formation with a heterogeneous carrier bed similar to that in panel D. However, the type III carrier is divided into two subtypes, where the average permeabilities are 0.1 md for the southern part and 0.01 md for the northern part. The color bar scale is the relative flux of migrated oil in pathways shown in panel B. Panels A and B are from Hindle (1997), and panels C to E are modified from Bekele et al. (1999), used with permission from the AAPG.

using a simple theoretical tube model of Dullien (1992):

$$\bar{r} = 2\sqrt{2k\tau/\phi} \qquad (3)$$

where k is the average permeability, ϕ is the average porosity, and τ is the tortuosity factor. The average permeability of the three types of carrier beds is 150 (type I), 10 (type II), and 0.1 (type III) md, as adapted from Bekele et al. (1999). The average porosity is taken as 15% (Matray and Chery, 1998), and the tortuosity factor is taken as 3 (Dullien, 1992). The pore-throat size is assumed to follow the Gaussian distribution; and the pore-throat radii are 0.05, 0.0125, and 0.0012 mm for types I, II, and III of carrier beds, respectively.

It is also assumed that hydrocarbons expelled from the Lower Jurassic source rocks entered directly into the overlying Middle Jurassic carrier beds and then migrated vertically upward within the carrier beds. Once reaching the base of the seal rock, hydrocarbons continued migrating along the top of Middle Jurassic carrier bed in the updip direction. Buoyancy force is designated as the driving force and capillary force as the resisting force. The intensity of hydrocarbon expulsion (Figure 8B) is adapted from Espitalié et al. (1988) and Bekele et al. (1999).

The superimposition of a structural map, localities of discovered oil fields, map of expulsion intensity, and simulated pathways in homogeneous carrier beds (Figure 8A–C) show that when the heterogeneity of the carrier is not taken into account, the simulation result (Figure 8C) is similar to those simulated with a flow path method by Hindle (1997). Nearly all discovered oil fields lie on or near the optimal pathways, except in the northern part of the basin, where simulated pathways are intensive but no oil field has been discovered.

However, results of simulations with a heterogeneous carrier (Figure 8D) also match well with the discovered hydrocarbon accumulations: Most oil fields lie on or near the optimal pathways. The correlation suggests that the pathways are principally controlled by the distribution of high-permeability carrier beds (Figure 8D) and by the intensity of hydrocarbon expulsion (Figure 8B). The number of pathways is high within the area of hydrocarbon expulsion, but pathways merge quickly with each other once outside of the expulsion area. Optimal pathways with a relatively large amount of migrated hydrocarbons are developed within the area of the high-permeability carrier bed (Figure 8D). In addition, the Bray fault (Figure 8A) is assumed to open for secondary migration. As a result, two optimal pathways form along the fault in the northwest-southeast orientation.

The simulation results also indicate that pathways in the northern part of the basin, where the carriers are tight (type III), are wide and intensive because the Bond number corresponding to type III carriers is smaller than that of the other types of carriers, following the relationships displayed in previous basin models (Figures 1–8).

Furthermore, if the expelling pressure δP in equation 2 is smaller than the average capillary pressure, which corresponds to a permeability smaller than 0.1 md, most of the oil may not be expelled from the source rock to the carrier. The simulation result (Figure 8E) indicates that the migrating oil was limited within the low-permeability carriers, the pathways did not merge to form optimal pathways, and as a result, no significant accumulations occurred. The simulation result supports the hypothesis that the low permeability of the carriers in the northern part hampered hydrocarbon migration and accumulation in that region.

DISCUSSION

Simulations in this study deal with only the simplest cases where oil migrates through a single carrier bed underneath a seal and do not consider pathway heterogeneity during vertical hydrocarbon migration. Pathways would merge and concentrate upsection during vertical migration (Hirsch and Thompson, 1995; Luo et al., 2007c), and their heterogeneity and efficiency in channeling hydrocarbon are significantly controlled by vertical heterogeneity of physical properties of carrier beds (Karlsen and Skeie, 2006). In fact, our simulations

are pseudo–3-D, and lateral migration in all simulations occurs in the top zone of carriers just underneath a perfect seal.

Physically, the invasion-percolation method seems similar to the flow path method (Shi, 2009) because in both methods migration is considered as the heterogeneous movement of hydrocarbon within a carrier toward an area with low flow potential. The migration process is compressed to an instant in both methods, that is, the temporal scaling effect is not considered. However, the techniques of calculation of hydrocarbon migration are different between the two methods.

In flow path methods, hydrocarbons can travel through carriers of any permeability as long as the driving force is large enough and/or the duration of migration is long enough (Dembicki and Anderson, 1989; Hindle, 1997; Shi, 2009) and the capillary pressure may be included in the flow potential (England et al., 1987; Hao et al., 2007). However, the spatial heterogeneity of a carrier is commonly effaced, whereas the carrier model was constructed with upscaling data (Welte et al., 2000). As a result, local variations in the physical properties of the carrier bed and some detailed properties of migration pathways cannot be explicitly presented (Carruthers, 2003; Luo, 2003; Shi, 2009).

Bekele et al. (1999) used a hybrid method, where the hydraulic formula based on Darcy's law was solved numerically to obtain the hydraulic head, and the hydrocarbon flow potential was calculated using Hubbert's (1953) equation. Based on the flow potential, the flow velocity and direction of oil phase were calculated. The method by Bekele et al. (1999) needs a long calculation time, and the number of sites in the carrier network is limited. As a result, their simulation results are of a low resolution (Hindle, 1999; Shi, 2009) without clearly defined migration pathways.

The relationship between the driving and resistant forces is critical to understanding the migration pathway development and is characterized by the dimensionless Bond number. The value of the Bond number is determined by not only the parameters in equation 1, but also implicitly the grid scale. The effect of the grid scale is similar to that of pore-throat size and has a power relation to the Bond number. This is an important characteristic of the invasion-percolation method in basin-scale migration simulation.

Many, if not most, cases of migration may arise from the combinations of scenarios modeled in this study. The simple simulations in this study are not exhaustive but can be used to demonstrate the fundamental characteristics and trends in pathway heterogeneity. The heterogeneity is controlled by heterogeneous carriers, flow-potential fields, source rock distributions, and hydrocarbon expulsion. Real migration processes are likely influenced by several controlling factors with varying complexities. The resulting heterogeneous migration pathways may or may not be the sum of basic trends as simulated in this study because nonlinear interactions and feedback most likely occur.

Our simulation indicates that a pathway, once intercepting a preexisting pathway, will merge with the preexisting pathway. This is because hydrocarbons will follow pathways that have the largest difference between driving and resisting forces (Hirsch and Thompson, 1995; Luo et al., 2004; Karlsen and Skeie, 2006), and preexisting pathways are places commonly with the least resistance.

For episodic migration processes, the preexistence of a network of pathways has, in fact, modified the originally macroscopically homogeneous carrier medium, which becomes heterogeneous to later migration. This type of heterogeneity may be exacerbated by the interaction and feedback mechanisms among pathways. Hydrocarbons migrating later through this medium will preferentially select the preexisting pathways. Moreover, the grain surface of the preexisting pathways has been modified/coated by previously migrated hydrocarbons (Dullien, 1992), resulting in a heterogeneously oil-wetted carrier. Finally, our physical migration experiments indicate that the initial pathways created by an initially weak driving force are commonly narrow but will not change until the weak force is increased several times (Hou et al., 2005). Even then, the widened pathways are much narrower than those formed initially by a large driving force.

Systematic experiments indicate that the fundamental cause of pathway heterogeneity is the

competition among pathways of different characteristics as caused by the microscopic heterogeneity of carrier media (Lenormand, 1985; Catalan et al., 1992; Tokunaga et al., 2000). The degree of pathway heterogeneity is mainly determined by the relative strength of the driving force to the resisting force (Tokunaga et al., 2000; Luo et al., 2004; Hou et al., 2005). All porous media are inherently microscopically heterogeneous (De Marsily, 1981; Weber, 1986); hence, pathway heterogeneity is intrinsic to the hydrocarbon migration process.

The heterogeneity of migration pathways in macroscopically homogeneous media is represented by not only the number and geometry of pathways themselves, but also the amount of migrated hydrocarbons through the pathways (Figures 1–8). This phenomenon reflects the control of preexisting pathways on a later migration (Luo et al., 2004, 2007b) and is illustrated in this study by the flux of migrated hydrocarbon in a pathway. This study demonstrates another kind of heterogeneity of migration, that is, the amount of migrated hydrocarbons in individual pathways differs significantly. It offers a potential method to assess the efficiency of pathways and to identify the optimal pathways for hydrocarbon migration.

CONCLUSIONS

Hydrocarbon migration in carriers is highly heterogeneous. Migration pathways are irregular and have a strong tendency to merge with each other to form optimal pathways. Pathway heterogeneity is caused fundamentally by microscopic heterogeneity of the physical properties of the carriers. The initial selection of pathways by migrating hydrocarbon is random. Later hydrocarbon migrates in preexisting pathways and further selects preferred pathways, resulting in a variable amount of migrated hydrocarbon in individual pathways and, ultimately, forming the optimal migration pathways.

The geometry and merging of pathways are determined by the ratio between the driving and resisting forces. In the case of a relatively large driving force, pathways tend to be thin and straight, perpendicular to the equipotential lines, with minimal merging. With a decreasing driving force, pathways widen, become more irregular, and merge commonly to form prominent amalgamated optimal pathways.

Macroscopic heterogeneity of carrier beds exacerbates pathway heterogeneity. Hydrocarbon tends to migrate toward and within carrier beds with a higher permeability and porosity, which will takeover low-permeability and low-porosity carrier beds as the dominant conduits of secondary migration. Migration pathways develop in and occupy first the high-permeability and high-porosity carrier beds, then extend into low-quality carrier beds. Large hydrocarbon accumulations should be associated with high-volume pathways.

The heterogeneity of carrier beds at variable scales exerts a stronger control on pathway heterogeneity than the driving force. A change in driving force, nevertheless, can still significantly change the characteristics of pathways. The control of carrier-bed heterogeneity decreases with increasing driving force, and pathways tend to be thin and straight and perpendicular to equipotential lines. In contrast, the control of carrier bed heterogeneity strengthens with decreasing driving force, and pathways tend to widen and become irregular.

The distribution and intensity of hydrocarbon expulsion from source rocks are spatially and temporally nonuniform in sedimentary basins, as caused by a variety of depositional, diagenetic, and structural processes. Source rock heterogeneity will cause highly heterogeneous pathway distributions and a variable amount of migrated hydrocarbons through the pathways.

REFERENCES CITED

Allen, P. A., and J. R. Allen, 1990, Basin analysis: Principles and applications, 2d ed.: Malden, Blackwell Publishing, 549 p.

Bekele, E., M. Person, and G. de Marsily, 1999, Petroleum migration pathways and charge concentration: A three-dimensional model: Discussion: AAPG Bulletin, v. 83, no. 6, p. 1015–1019.

Berg, R. R., 1975, Capillary pressure in stratigraphic traps: AAPG Bulletin, v. 59, no. 6, p. 939–959.

Bo, Z., D. Loggia, L. Xiaorong, G. Vasseur, and H. Ping, 2006, Numerical studies of gravity destabilized percolation in

2-D porous media: The European Physical Journal B, v. 50, no. 4, p. 631–637, doi:10.1140/epjb/e2006-00168-y.
Carruthers, D. J., 2003, Modeling of secondary petroleum migration using invasion percolation techniques, *in* S. Duppenbecker and R. Marzi, eds., Multidimensional basin modeling: AAPG/Datapages Discovery Series 7, p. 21–37.
Catalan, L., W. F. Xiao, I. Chatzis, and F. A. L. Dullien, 1992, An experimental study of secondary oil migration: AAPG Bulletin, v. 76, no. 5, p. 638–650.
Chapman, R. E., 1982, Effects of oil and gas accumulation on water movement: AAPG Bulletin, v. 66, no. 3, p. 2179–2183.
Chiarelli, A., 1973, Etude des nappes aquifères profondes, contribution de l'hydrogéologie a la reconnaissance d' un bassin sédimentaire at à l'exploration pétrolière: Société National Elf Aquitaine (production), 187 p.
De Marsily, G., 1981, Hydrogéologie quantitative: Paris, Masson, 215 p.
Dembicki, H. J., and M. J. Anderson, 1989, Secondary migration of oil: Experiments supporting efficient movement of separate, buoyant oil phase along limited conduits: AAPG Bulletin, v. 73, no. 8, p. 1018–1021.
Dullien, F. A. L., 1992, Porous media: Fluid transport and pore structure, 2d ed.: San Diego, Academic Press, p. 1–332.
England, W. A., A. S. Mackenzie, D. M. Mann, and T. M. Quigley, 1987, The movement and entrapment of petroleum fluids in the subsurface: Geological Society (London) Special Publication 114, p. 327–347.
Espitalié, J., J. R. Maxwell, Y. Chenet, and F. Marquis, 1988, Aspects of hydrocarbon migration in the Paris Basin as deduced from organic geochemical survey, *in* L. Mattavelli and L. Novelli, eds., Advances in organic geochemistry 1987: Organic Geochemistry, v. 13, p. 467–481, doi:10.1016/0146-6380(88)90068-X.
Ewing, R. E., 1997, Aspects of upscaling in simulation of flow in porous media: Advances in Water Resources, v. 20, no. 5–6, p. 349–358, doi:10.1016/S0309-1708(96)00052-8.
Furuberg, L., J. Feder, A. Aharony, and T. Jøssang, 1988, Dynamics of invasion percolation: Physical Review Letters, v. 61, p. 2117–2120.
Hantschel, T., and A. I. Kauerauf, 2009, Fundamentals of basin and petroleum systems modeling: Dordrecht, Heidelberg, Springer, 476 p.
Hao, F., H. Y. Zou, Z. S. Gong, and Y. H. Deng, 2007, Petroleum migration and accumulation in the Bozhong Subbasin, Bohai Bay Basin, China: Significance of preferential petroleum migration pathways (PPMP) for the formation of large oil fields in lacustrine fault basins: Marine and Petroleum Geology, v. 24, no. 1, p. 1–13, doi:10.1016/j.marpetgeo.2006.10.007.
Hao, F., X. H. Zhou, Y. M. Zhu, and Y. Y. Yang, 2009, Mechanisms for oil depletion and enrichment on the Shijiutuo uplift, Bohai Bay Basin, China: AAPG Bulletin, v. 93, no. 8, p. 1015–1037, doi:10.1306/04140908156.
Harms, J. C., 1966, Stratigraphic traps in a valley fill, western Nebraska: AAPG Bulletin, v. 50, no. 10, p. 2119–2149.
Hindle, A. D., 1997, Petroleum migration pathways and charge concentration: A three-dimensional model: AAPG Bulletin, v. 81, no. 9, p. 1451–1481.
Hindle, A. D., 1999, Petroleum migration pathways and charge concentration: A three-dimensional model: Reply: AAPG Bulletin, v. 83, no. 6, p. 1020–1023.
Hirsch, L. M., and A. H. Thompson, 1995, Minimum saturations and buoyancy in secondary migration: AAPG Bulletin, v. 79, no. 5, p. 696–710.
Hou, P., B. Zhou, and X. R. Luo, 2005, Experimental studies on pathway patterns of secondary oil migration: Science in China Series D, v. 49, no. 2, p. 469–473.
Hubbert, M. K., 1953, Entrapment of petroleum under hydrodynamic conditions: AAPG Bulletin, v. 37, no. 8, p. 1954–2026.
Karlsen, D. A., and J. E. Skeie, 2006, Petroleum migration, faults and overpressure: Part I. Calibrating basin modeling using petroleum in traps: A review: Journal of Petroleum Geology, v. 29, no. 3, p. 227–256, doi:10.1111/j.1747-5457.2006.00227.x.
Lehner, F. K., D. Marsal, L. Hermans, and A. van Kuyk, 1988, A model of secondary migration as a buoyancy-driven separate phase flow: Revue de l'Institut Français du Pétrole, v. 43, p. 155–164.
Lenormand, R., 1985, Differents mécanismes de déplacements visqueux et capillaries en millieux poreux: Comptes Rendus de l'Académie des Sciences, Paris II, v. 301, p. 247–250.
Lenormand, R., E. Touboul, and C. Zarcone, 1988, Numerical models and experiments on immiscible displacements in porous media: Journal of Fluid Mechanics, v. 189, p. 165–187, doi:10.1017/S0022112088000953.
Luo, X. R., 2003, Review of hydrocarbon migration and accumulation dynamics (in Chinese): Natural Gas Geoscience, v. 14, no. 5, p. 337–346.
Luo, X. R., F. Q. Zhang, S. Miao, W. M. Wang, Y. Z. Huang, D. Loggia, and G. Vasseur, 2004, Experimental verification of oil saturation and loss during secondary migration: Journal of Petroleum Geology, v. 27, no. 3, p. 241–251, doi:10.1111/j.1747-5457.2004.tb00057.x.
Luo, X. R., L. K. Zhang, Q. J. Liao, J. Q. Su, S. Q. Yuan, H. M. Song, B. Zhou, and P. Hou, 2007a, Simulation of hydrocarbon migration dynamics in Shahejie Formation of Chengbei fault step zone: Oil & Gas Geology, v. 28, no. 2, p. 191–197.
Luo, X. R., J. Yu, L. Q. Zhang, Y. Yang, R. Y. Chen, Z. K. Chen, and B. Zhou, 2007b, Numerical modeling of secondary migration and its applications to Chang-6 Member of Yanchang Formation (Upper Triassic), Longdong area, Ordos Basin: China Science in China Series D, v. 50, no. 2, p. 91–102.
Luo, X. R., B. Zhou, S. X. Zhao, F. Q. Zhang, and G. Vasseur, 2007c, Quantitative estimates of oil losses during migration: Part I. The saturation of pathways in carrier beds: Journal of Petroleum Geology, v. 30, no. 4, p. 375–387, doi:10.1111/j.1747-5457.2007.00375.x.
Magara, K., 1978, Compaction and fluid migration, Practical petroleum geology: Amsterdam, Elsevier, 319 p.
Mann, U., 1997, Petroleum migration: Mechanisms, pathways, efficiencies and numerical simulations, *in* D. H.

Welte and D. R. Baker, eds., Petroleum and basin evolution: Berlin, Germany, Springer-Verlag, p. 405–520.
Matray, J. M., and L. Chery, 1998, Origin and age of deep waters of the Paris Basin, *in* C. Causse and F. Gasse, eds., Hydrologie et géochimie isotopique: Paris, France, Editions de l'ORSTOM, p. 117–133.
McAuliffe, C. D., 1979, Oil and gas migration: Chemical and physical constraints: AAPG Bulletin, v. 63, no. 5, p. 767–781.
McNeal, R. P., 1961, Hydrodynamic entrapment of oil and gas in Bisti field, San Juan County, New Mexico: AAPG Bulletin, v. 45, no. 3, p. 315–329.
Meakin, P., G. Wagner, A. Vedvik, H. Amundsen, J. Feder, and T. Jùssang, 2000, Invasion percolation and secondary migration: Experiments and simulations: Marine and Petroleum Geology, v. 17, no. 7, p. 777–795, doi:10.1016/S0264-8172(99)00069-0.
Pages, L., 1987, Exploration of the Paris Basin, *in* J. Brooks and K. Glennie, eds., Petroleum geology of north west Europe: London, Graham and Trotman, p. 87–93.
Philip, Z. G., J. W. Jennings Jr., J. E. Olson, S. E. Laubach, and J. Holder, 2005, Modeling coupled fracture-matrix fluid flow in geomechanically simulated fracture networks: Society of Petroleum Engineers Reservoir Evaluation & Engineering, v. 8, no. 4, p. 300–309.
Pratsch, J. C., 1983, Gasfields, NW German Basin: Secondary migration as a major geologic parameter: Journal of Petroleum Geology, v. 5, no. 3, p. 229–244, doi:10.1111/j.1747-5457.1983.tb00569.x.
Schowalter, T. T., 1979, Mechanics of secondary hydrocarbon migration and entrapment: AAPG Bulletin, v. 63, no. 5, p. 723–760.
Shi, G. R., 2009, Status, problems and proposals of the quantitative modeling techniques for hydrocarbon migration and accumulation: Oil & Gas Geology, v. 30, no. 1, p. 1–10.
Smith, D. A., 1966, Theoretical considerations of sealing and non-sealing faults: AAPG Bulletin, v. 50, no. 2, p. 363–374.
Sylta, Ø., 1991, Modeling of secondary migration and entrapment of a multicomponent hydrocarbon mixture using equation of state and ray-tracing modeling techniques: Geological Society (London) Special Publication 59, p. 111–122.
Thomas, M. M., and J. A. Clouse, 1995, Scaled physical model of secondary oil migration: AAPG Bulletin, v. 79, no. 1, p. 19–29.
Tokunaga, T., K. Mogi, O. Matsubara, H. Tosaka, and K. Kojima, 2000, Buoyancy and interfacial force effects on two-phase displacement patterns: An experimental study: AAPG Bulletin, v. 84, no. 1, p. 65–74.
Ungerer, P., J. Burrus, B. Doligez, Y. Chenet, and F. Bessis, 1990, Basin evaluation by integrated two-dimensional modeling of heat transfer, fluid flow, hydrocarbon generation, and migration: AAPG Bulletin, v. 74, no. 3, p. 309–335.
Weber, K. J., 1986, How heterogeneity affects oil recovery, *in* L. W. Lake and H. B. Carroll, Jr., eds., Reservoir characterization: New York, Academic Press, p. 487–544.
Welte, D. H., T. Hantschel, B. P. Wygrala, K. S. Weissenburger, and D. Carruthers, 2000, Aspects of petroleum migration modeling: Journal of Geochemical Exploration, v. 69–70, p. 711–714, doi:10.1016/S0375-6742(00)00105-9.
Wilkinson, D., 1986, Percolation effects in immiscible displacement: Physical Review A, v. 34, p. 1380–1391.
Wilkinson, D., and J. F. Willemsen, 1983, Invasion percolation: A new form of percolation theory: Journal of Physics, v. A16, p. 3365–3376.
Zhang, F. Q., X. R. Luo, S. Miao, W. M. Wang, B. Zhou, and Y. Z. Huang, 2003, The patterns and its effect factors of secondary hydrocarbon migration (in Chinese): Petroleum Geology & Experiment, v. 25, no. 1, p. 69–75.